www.nature.com/modpathol

ARTICLE

Senescence markers in focal nodular hyperplasia of the liver: pathogenic considerations on the basis of immunohistochemical results

Helmut Denk[1] ✉, Daniela Pabst[1], Peter M. Abuja[1], Robert Reihs[1], Brigitte Tessaro[1], Kurt Zatloukal[1] and Carolin Lackner[1]

Focal nodular hyperplasia (FNH) is a polyclonal tumour-like hepatic lesion characterised by parenchymal nodules, connective tissue septa without interlobular bile ducts, pronounced ductular reaction and inflammation. It may represent a response to local arterial hyperperfusion and hyperoxygenation resulting in oxidative stress. We aimed at obtaining closer insight into the pathogenesis of FNH with its characteristic morphologic features. Immunohistochemistry and immunofluorescence microscopy was performed on FNH specimens using antibodies against keratins (K) 7 and 19, neural cell adhesion molecule (NCAM), lamin B1, senescence markers (CDK inhibitor 1/p21^{Cip1}, CDK inhibitor /p16^{Ink4a}, senescence-associated (SA) β- galactosidase activity), proliferation markers (Ki-67, proliferating-cell nuclear antigen (PCNA)), and the abnormally phosphorylated histone γ-H2AX, indicating DNA double strand breaks; moreover SA β- galactosidase activity was determined histochemically. Ductular metaplasia of hepatocytes indicated by K7 expression in the absence of K19 plays a major role in the development of ductular reaction in FNH. Moreover, the expression of senescence markers (p21^{Cip1}, p16^{Ink4a}, γ-H2AX, SA β-galactosidase activity) in hepatocytes and cholangiocytes suggests that stress-induced cellular senescence contributes to fibrosis and inflammation via production of components of the senescence-associated secretory phenotype. Expression of proliferation markers (Ki-67, PCNA) was not enhanced in hepatocytes and biliary cells. Senescence and ductular metaplasia of hepatocytes may thus be involved in inflammation, fibrosis and apoptosis resistance. Hence, fibrosis, inflammation and reduced apoptotic cell death, rather than proliferation (hyperplasia) may be responsible for increased tissue mass and tumour-like appearance of FNH.

Modern Pathology (2022) 35:87–95; https://doi.org/10.1038/s41379-021-00940-5

INTRODUCTION

Focal nodular hyperplasia (FNH) is a polyclonal tumour-like lesion in the liver with an incidence of about 0.8% in autopsy series. 80–90% of FNHs are discovered in women in their 3rd to 4th decades. They are mostly solitary, clinically asymptomatic incidental findings and may regress with age[1–5]. The lesion is regarded as hyperplastic response to local arterial hyperperfusion and hyperoxygenation[1,2,6]. mRNA expression levels of the angiopoietin genes (*ANGPT1* and *2*) involved in vessel maturation and the *ANGPT1:ANGPT2* ratio are increased in comparison to normal liver, liver neoplasms and cirrhosis[7].

Aim of the present study was to shed further light on the pathogenesis of morphologic features characteristic of FNH. Moreover, this lesion may also serve as a model regarding origin and significance of pronounced ductular reaction (DR) with its associated inflammation and fibrosis. The results obtained suggest that cellular senescence of hepatocytes and ductular cholangiocytes plays a major pathogenic role.

MATERIAL AND METHODS

Sixteen surgically removed FNH specimens were selected from the archive of the Institute of Pathology, Medical University of Graz, Austria (patient characteristics are listed in Table 1). The study was approved by the Ethics Committee of the Medical University of Graz, Austria. The tissues were fixed in 10% buffered formalin and embedded in paraffin by routine procedures; 5 µm thick sections were stained after removal of paraffin with hematoxylin-eosin (H&E) and chromotrope aniline blue (CAB) for light microscopy and subjected to immunohistochemistry. In addition, immunofluorescence microscopy was performed on 5 µm thick acetone-fixed sections of frozen material of one FNH specimen with adjacent normal liver tissue. Sections were examined by two board-certified pathologists (H.D., C. L.). Details concerning antigens to be detected and immunohistochemical and immunofluorescence procedures are listed in Supplementary Table 1.

For grading of keratin (K) 7 expression in hepatocytes (K7-positive/K19-negative hepatocytes) and DR the method proposed by Yabushita et al.[8] was modified (grade 1: only K7-positive DR; grade 2: in addition to K7-positive DR, periportal hepatocytes are K7-positive; grade 3: in addition to periportal K7-positive hepatocytes also intranodular hepatocytes are K7-positive; since the association of K7-positive/K19-negative hepatocytes with FNH nodules was variable, the parenchymal areas with the most prominent immune reaction were graded).

Senescence-associated (SA) β-galactosidase was determined histochemically in frozen sections according to the protocol provided by the company (Supplementary Table 1).

For quantification of nuclear CDK inhibitor 1/p21^{Cip1} (p21), proliferating cell nuclear antigen (PCNA) and Ki-67 expression in FNH versus normal liver, the immunostained slides were scanned with the 3DHistech P1000 scanner

[1]Diagnostic & Research Centre of Molecular Biomedicine, Institute of Pathology, Medical University of Graz, Graz, Austria. ✉email: helmut.denk@medunigraz.at

Received: 8 July 2021 Revised: 23 September 2021 Accepted: 23 September 2021
Published online: 13 October 2021

Table 1. Patient characteristics, presence of K7-positive hepatocytes in relation to DR (graded according to Yabushita et al.[8]), percentage of Ki-67- and PCNA-positive cells.

Patient No.	Gender (male/female)	Age (years)	K7 grade	% Ki-67-positive cells in FNH (in normal tissue)	% PCNA-positive cells in FNH (in normal tissue)
1	m	36	1	0.11 (0.12)	0.05 (0.01)
2	m	24	1	0.02 (–)	0.09 (–)
3	f	23	2	1.18 (–)	0.22 (–)
4	f	46	2	0.39 (–)	0.17 (–)
5	f	25	3	1.44 (1.68)	0.19 (0.25)
6	f	43	1	0.22 (0.28)	0.01 (0.13)
7	f	25	1	0.33 (0.59)	0.05 (0.06)
8	f	44	1	0.23 (0.24)	0.31 (0.12)
9	f	22	1	0.16 (0.20)	0.13 (0.08)
10	f	43	3	0.33 (0.40)	0.39 (0.53)
11	f	23	2	1.02 (0.99)	0.10 (0.14)
12	f	52	3	0.36 (0.47)	0.19 (0.14)
13	f	40	3	0.17 (0.25)	0.08 (0.01)
14	f	29	1	0.52 (0.64)	0.16 (0.06)
15	m	43	1	0.34 (0.70)	0.59 (0.04)
16	f	25	2	0.26 (0.26)	0.24 (0.44)

Mean percentage of Ki-67-positive cells: 0.44% in FNH, 0.53% in normal tissue; mean percentage of PCNA-positive cells 0.18% in FNH, 0.16% in normal tissue.
(–), no normal tissue present.

(3DHISTECH Ltd., Budapest, Hungary). All analyses were performed with QuPath 0.2.3[9]. For cell counting, the 'positive cell detection' algorithm from QuPath was used and the percentages of positive and negative hepatocytes were calculated in FNH and surrounding normal liver tissue. Significance of p21 expression was assessed with R 3.6.2[10,11] and the *p* values were calculated with the Wilcoxon Signed Rank Test.

RESULTS

Light microscopy

The FNHs studied were circumscribed but not encapsulated multinodular lesions which displayed characteristic and already well described morphologic features with fibrous septa, DR and chronic inflammation[2,3]. The parenchymal nodules were separated by connective tissue septa. Often a larger central fibrotic scar with radiating branches, reminiscent of portal tracts but lacking interlobular bile ducts, was present. The nodules varied in size and shape; the hepatocytes were arranged in one- or two- cell- thick plates. In some areas of most FNHs, small groups of hepatocytes or single hepatocytes in association with ductules, similar to hepatocyte buds as described in cirrhosis by Stueck and Wanless[12], were seen. Focally, sinusoids within the nodules were dilated and some vascular spaces were reminiscent of central veins. In most cases, the hepatocytes showed mild to moderate degree of macrovesicular steatosis and mild variations in cell and nuclear size. Their lipofuscin content did not differ from that of the hepatocytes of the surrounding normal liver. Mitoses were absent. In one case (No. 12 in Table 1), at the periphery of nodules enlarged and rounded (ballooned) hepatocytes with lightly stained cytoplasm, some of which contained Mallory-Denk bodies (MDBs), were observed. These features were not present in the surrounding liver which showed only moderate macrovesicular steatosis. Scars and septa were infiltrated to a variable degree mostly by lymphocytes with occasional follicular arrangement. Septa contained middle-sized and larger vessels with irregular, often fibrohyalinized, walls, particularly with thickening of the intima; vessels with obliterated lumina were also seen. Occasionally, densely arranged, small to middle-sized, regularly structured arteries almost completely filled the connective tissue space. Some thin-walled vessels in continuity with dilated sinusoids were reminiscent of portal vein branches. Moreover, small endothelium-lined vascular spaces with dilated lumina, possibly resembling lymphatics, were observed. DR occupied to various extent the interface between connective tissue and parenchyma, focally protruding into the nodule. The ductules were mostly arranged in solid, sometimes branching cords or displayed discrete slit-like lumina; however, some ductules showed dilated lumina lined by flat and atrophic, but occasionally also cuboidal epithelium similar to interlobular bile ducts, possibly resembling a maturation process. In some areas, the parenchyma at the nodular periphery was dissociated by ductules with associated inflammation and fibrosis and the impression was gained, that larger nodules may be dissected into smaller ones by this process. Some nodules were partially surrounded by elongated ductules (ductal plate-like) as usually seen in cirrhosis. The liver outside the lesion showed no major architectural abnormalities with regularly arranged hepatocytes, occasional macrovesicular steatosis, usually mild lymphocytic infiltration of portal tracts containing interlobular bile ducts and sometimes slightly elongated ductules. Larger arteries, veins and bile ducts were often seen in fibrotic liver tissue in the immediate vicinity of FNH.

Immunohistochemistry

A variable number of normal-sized and -shaped FNH-associated hepatocytes showed cytoplasmic K7-specific immunostaining (without its partner K19; i.e., K7-positive/K19-negative hepatocytes), although with weaker intensity than cholangiocytes of the DR (Table 1; Figs. 1, 2); the staining was accentuated at the cell periphery, in line with increased density of the intermediate filament cytoskeleton at this position, indicating that K7 forms intermediate filaments with K18 as partner. These hepatocytes mostly occupied the nodular periphery adjacent to, and merging with, the DR (Figs. 1, 2). Their arrangement closely resembled hepatocyte plates ('muralia'[13]), although somewhat distorted by fibrosis and inflammation, and was thus consistent with ductular metaplasia (transdifferentiation) of hepatocytes[14–17]. The number of K7-positive/K19-negative hepatocytes in the nodules varied from rare to numerous in different FNHs (see Table 1), but also within a single specimen. We observed a continuous decrease in cellular size from K7-positive hepatocytes towards K7-positive ductular cells, and this was

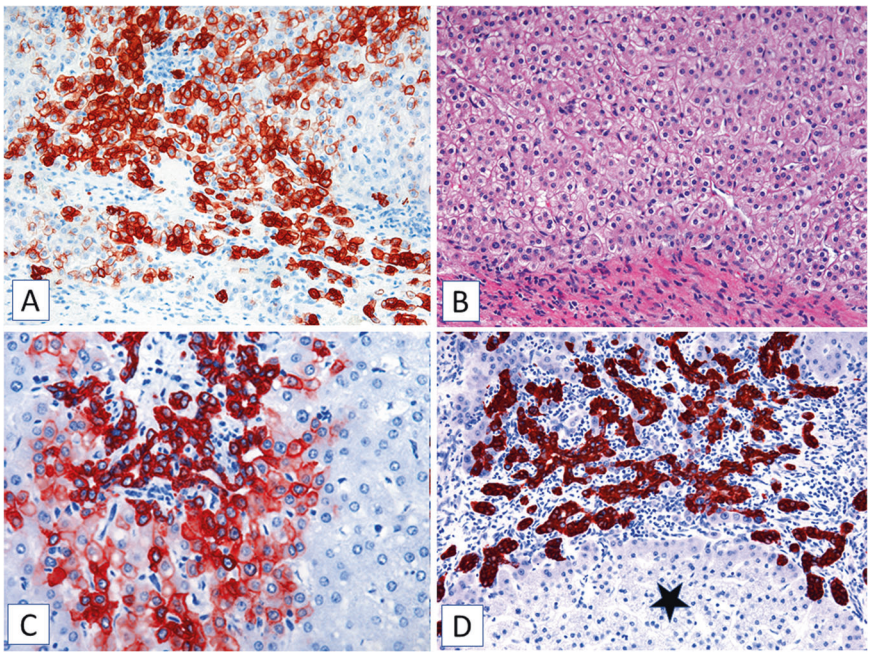

Fig. 1 Different stages of ductular metaplasia in FNH (immunohistochemistry using antibodies to K7). A Numerous K7-positive hepatocytes present in a FNH nodule. **B** Corresponding field in a consecutive H&E-stained section showing morphology and arrangement of hepatocytes. **C** K7-positive hepatocytes arranged in plates are in continuity with ductules (interpreted as progressing stage of ductular metaplasia). **D** Ductular reaction with inflammatory infiltrate without association with K7-positive hepatocytes (possible final stage of ductular metaplasia; asterisk indicates nodular parenchyma).

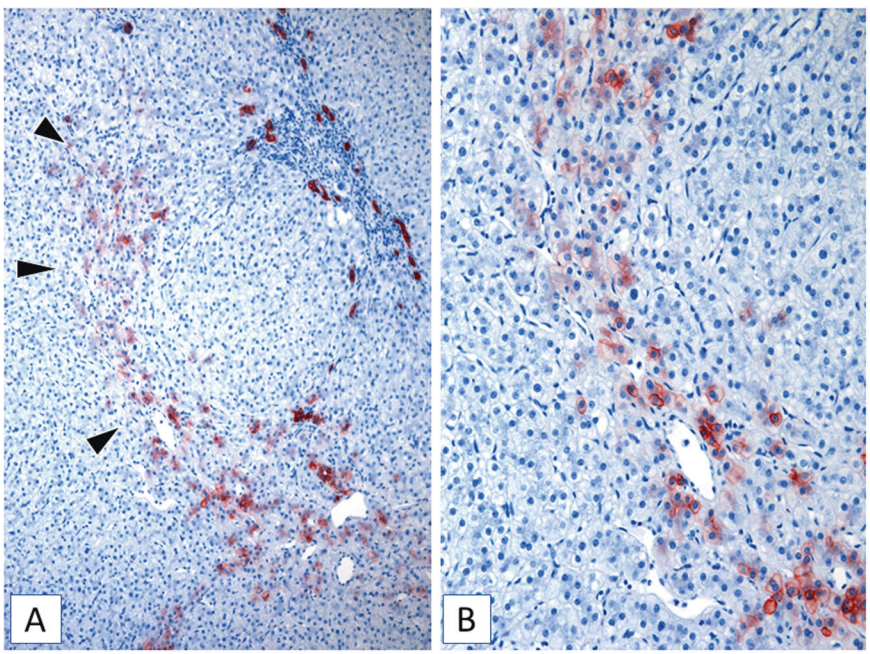

Fig. 2 Immunohistochemistry using antibodies to K7 (FNH). A K7-positive hepatocytes aligned in a file associated with inflammation and fibrosis suggesting an early stage of septum and nodule formation (arrow-heads). Higher magnification in (**B**).

correlated with increased intensity of K7 immunoreactivity (Fig. 1C). In addition, K7-positive single hepatocytes or small groups were also present within nodules distant from DR. Some small nodules were even completely K7-positive without clear-cut spatial relationship to DR. Occasionally, K7-positive/K19-negative hepatocytes were arranged in single files suggesting an early stage of septum formation with dissection of nodules into smaller units (Fig. 2A, B). K19-positive hepatocytes were absent in FNH. Coexpression of K7 and K19 only occurred in cells resembling ductular epithelium. However, ductular morphology was not consistently associated with K7/K19 coexpression since the number of K7-positive ductular cells clearly exceeded K7/K19-positive ones. The latter usually displayed distinct lumina whereas ductular elements in closer vicinity to the parenchyma were more often K19-negative. Hepatocytes in 'bud'-like arrangement[12] were K7-negative in contrast to the surrounding ductules (Fig. 3). In the surrounding normal liver K7-positive/

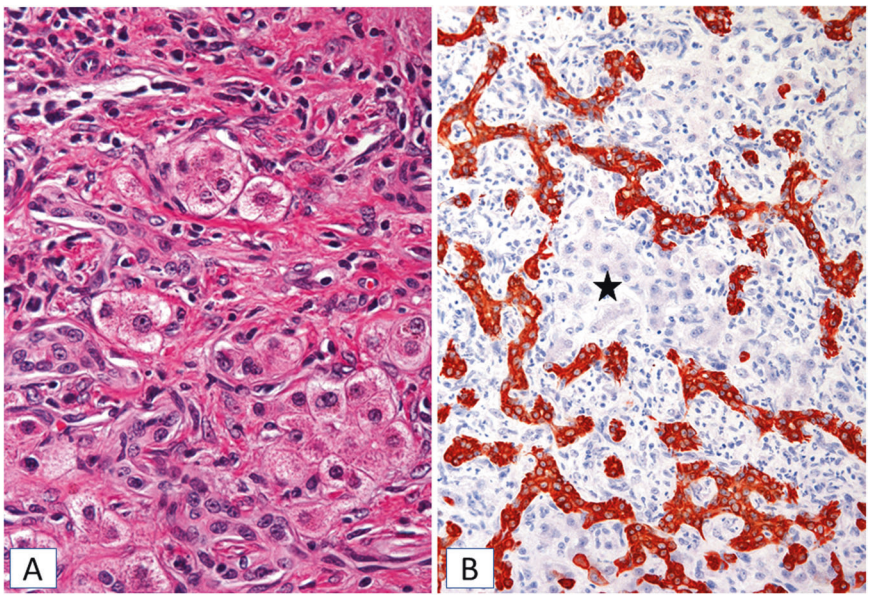

Fig. 3 Bud-like arrangement of hepatocytes in association with ductules in FNH. A Bud-like arrangement of hepatocytes in association with ductules (H&E). **B** Irregularly arranged anastomosing ductules expressing K7 (immunohistochemistry using antibodies to K7) surround small groups of K7-negative hepatocytes (asterisk).

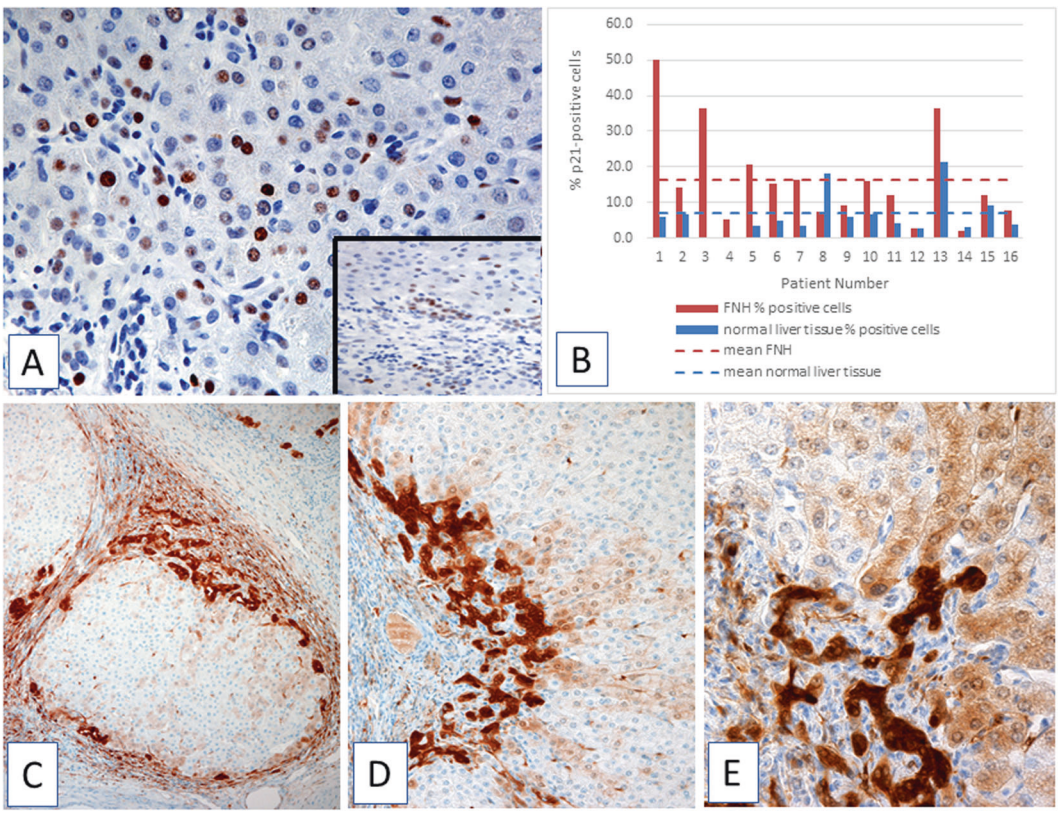

Fig. 4 Expression of p21 and p16 in hepatocytes and ductules. A Hepatocytes and ductules (inset) in FNH contain p21- positive nuclei (immunohistochemistry using antibodies to p21). **B** Quantification of p21- positive cells in FNHs and normal liver tissues (FNH: mean 16.46 ± SD 3.47; normal liver tissue: mean 7.12 ± SD 5.67; $p = 0.014$) **C**–**E** Immunohistochemistry using antibodies to p16. **C** FNH nodule partially surrounded by p16-positive DR; positive spindle cells are present in the septum. **D** p16-positive DR and weaker cytoplasmic and nuclear p16-positivity of adjacent hepatocytes. **E** Plates of p16-positive hepatocytes merging with positive ductules.

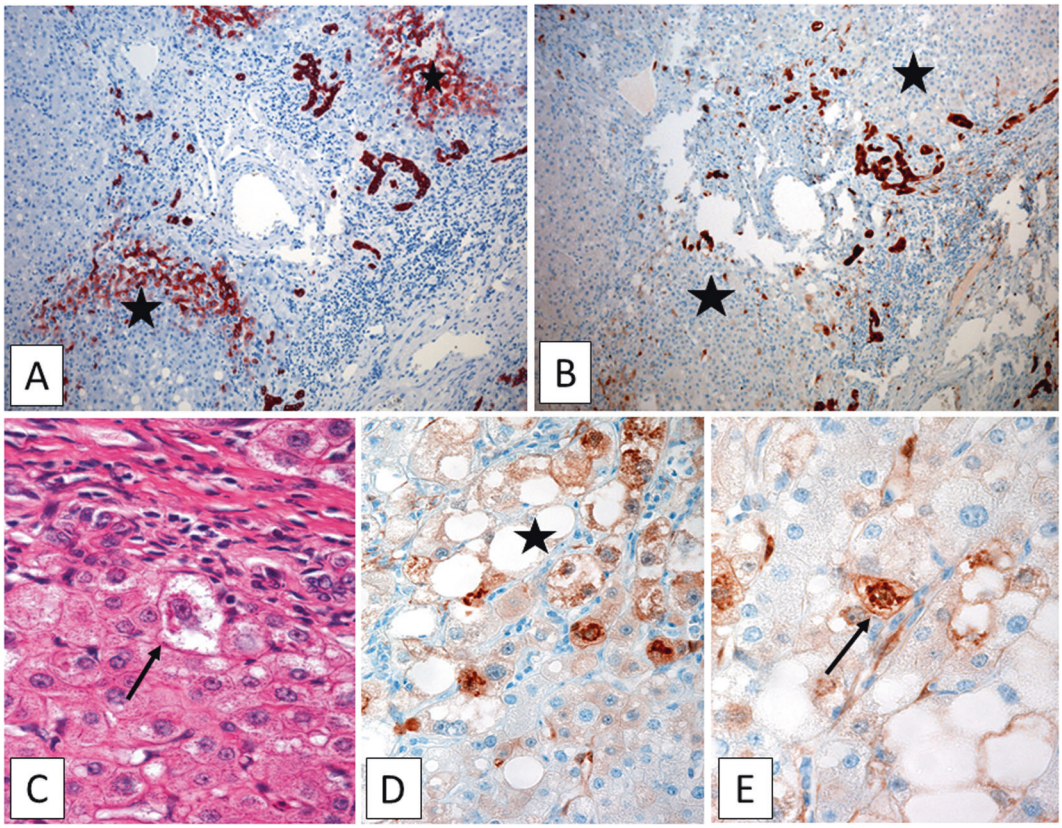

Fig. 5 Expression of K7 and p16 in hepatocytes and ductules of FNH. A, **B** Comparison of K7 and p16 expression in FNH (immunohistochemistry using antibodies to K7 (**A**) and p16 (**B**), respectively, in consecutive sections). Antibodies to K7 (**A**) react in addition to ductules with hepatocytes in circumscribed areas (asterisks), whereas p16 antibodies (**B**) decorate only ductular cells. **C** Ballooned hepatocyte with MDB (arrow; H&E). **D** Macrovesicular steatosis and group of ballooned hepatocytes (asterisk) expressing cytoplasmic and nuclear p16 and containing p16-positive MDBs. **E** MDB-containing p16-positive hepatocyte is shown at higher magnification (arrow).

K19-negative hepatocytes were absent (except in one case), and K7/K19 coexpression was restricted to interlobular bile ducts and ductules. In one case (No. 5 in Table 1), normal liver in proximity to FNH contained small groups of K7-positive/K19-negative hepatocytes adjacent to ductules in acinar zone 1.

In the majority of FNHs, numerous hepatocytes, with preference of the nodular periphery and subcapsular regions, as well as ductular epithelial cells expressed nuclear p21 (Fig. 4A, B). In most normal livers, p21- positive hepatocytes were significantly less frequent. Only in two cases (patients No. 8 and 14) the percentage of p21-positive hepatocytes in normal liver exceeded that in FNH (Fig. 4B). Interlobular bile ducts in normal liver contained p21-expressing epithelial cells in variable numbers.

The epithelial cells of the FNH-associated DR consistently expressed nuclear and cytoplasmic CDK inhibitor 2/p16^{Ink4a} (p16) (Figs. 4, 5). A weaker p16 immunostaining was also a feature of hepatocytes, mostly in continuity with the DR (Fig. 4C–E). However, p16-positive hepatocytes without relationship to DR were also present in some nodules. Although overlap between p16- and K7- expressing hepatocytes occurred, p16 positivity was not consistently associated with K7 expression (Fig. 5A, B). MDBs were decorated by p16 antibodies in addition to the harbouring hepatocytes (Fig. 5C–E). p16-positive, mostly spindle-shaped perisinusoidal cells as well as mesenchymal cells in the connective tissue surrounding the nodules were observed (Fig. 4C). In normal liver, hepatocytes, bile ducts, ductules, and mesenchymal cells in the portal tracts were p16-negative (Fig. 6A), whereas spindle-shaped perisinusoidal cells were present in variable numbers. A microhamartoma (Von Meyenburg complex) in the surrounding liver contained few p16-positive cholangiocytes (Fig. 6B, C). Thus, p16 immunostaining allowed a clear-cut separation of FNH and normal liver.

Neural cell adhesion molecule (NCAM) antibodies decorated ductular cells of the DR in FNH, but not bile ducts of normal liver (Fig. 6D, E).

Ki-67-expressing hepatocytes and ductular cells were rare in FNH as well as in normal liver, whereas Ki-67 positive nuclei in inflammatory infiltrates and sinusoidal cells served as positive controls. Nuclear PCNA staining of hepatocytes and ductular cells in FNH was also rare but, if present, more frequent at the nodular periphery and in subcapsular regions. In normal liver, the frequency of PCNA-positive hepatocytes, interlobular bile ducts and ductules was also variable, but not different from FNH (Table 1).

In frozen sections of FNH in contrast to normal liver, antibodies to γ-H2AX (Ser139) revealed pronounced granular nuclear staining mostly of ductular cells, whereas only few surrounding hepatocytes displayed positive nuclei (Fig. 7A, B). Nuclei of hepatocytes and cholangiocytes were immunostained by lamin B1 antibodies in FNH (Fig. 7C) as well as normal liver.

In FNH, SA β-galactosidase histochemistry revealed distinct blue granular and needle-like precipitates predominantly in association with cholangiocytes (Fig. 7D, E) of the DR indicating activity of this enzyme variant as sign of senescence, whereas hepatocytes, bile ducts and ductules of normal liver were negative.

DISCUSSION

Morphologically, FNH resembles abnormally structured liver tissue, particularly rich in abnormal blood vessels and DR, but lacking

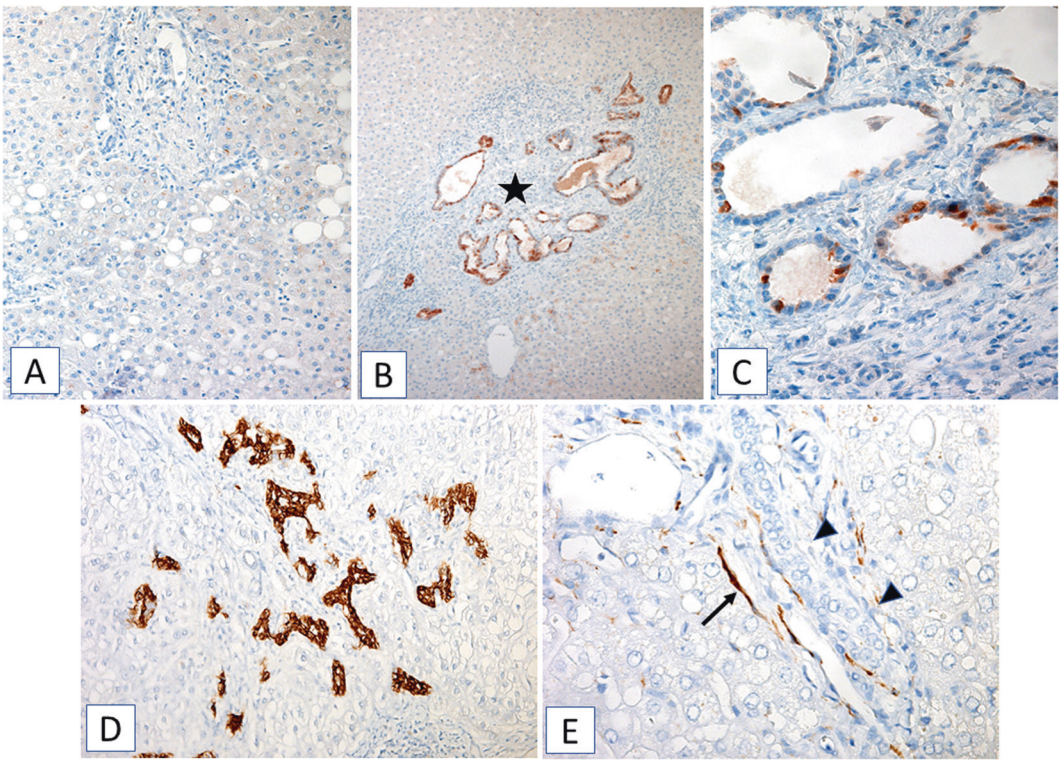

Fig. 6 Immunohistochemistry of normal liver and FNH using antibodies to p16 and NCAM. A Immunohistochemistry using antibodies to p16: hepatocytes and bile ducts of normal liver are negative for p16. **B**, **C** Microhamartoma (Von Meyenburg complex; asterisk) present in normal liver contains some p16-positive cholangiocytes (higher magnification shown in **C**). **D** Immunohistochemistry using antibodies to NCAM: cells of DR in FNH express NCAM. **E** In normal liver bile ducts (arrow-heads) are NCAM-negative. A positive reaction is seen in nerve fibers (arrow) serving as control.

typical portal tracts with interlobular bile ducts[2,3]. Arterial hyperperfusion is regarded responsible for hyperoxygenation and resulting oxidative stress as was also immunohistochemically demonstrated by the appearance of the oxidative stress marker 8-hydroxy-2′-deoxyguanosine (8-OHdG)[1,18,19]. Hepatic stellate cell activation by reactive oxygen species (ROS) may contribute to fibrosis and scarring[19]. The pronounced nuclear positivity for γ-H2AX (Ser139) in FNH-associated DR underlines the presence of a DNA damage response resulting from oxidative stress[20,21].

The significance and pathogenesis of the pronounced DR in FNH has been debated[17,22,23]. DR accompanies a variety of chronic liver diseases; since it is intimately associated with fibrosis and inflammation it may be a driver of disease progression[8,24–29] (cf.[29] for further references and information). As discussed by Desmet[14,15], three different types of DR can be distinguished on the basis of morphology and disease association: type I, mainly associated with bile duct obstruction consists of elongated pre-existing ductules, type II results from ductular metaplasia (transdifferentiation) of hepatocytes, and type III reflects activation and proliferation of hepatic progenitor cells. In the early stage of type II DR, normal-sized hepatocytes express (in addition to K8 and K18) K7 without co-expression of K19. With ongoing transformation of hepatocytes to the cholangiocyte phenotype, K19 appears in addition[14,15,17,29,30]. The epithelia in type II DR are arranged in irregular anastomosing strands vaguely reminiscent of hepatocyte plates[14–17,22,31]. Phenotypic transformation of mature hepatocytes to cholangiocytes has also been shown in animal as well as in cell culture experiments[32–35,28,35].

In previous reports, ductular metaplasia of hepatocytes was proposed to be responsible for DR in FNH[17,31,36]. Van Eyken et al.[17] observed a variable number of juxtaseptal K7-positive hepatocytes in close proximity to ductules. According to Iyer et al.[36], K7 expression by hepatocytes in FNH was less pronounced and absent in centrinodular position. Our immunohistochemical results support these findings since we also observed variable numbers of K7-positive hepatocytes, from absent to numerous, in close proximity to DR, but occasionally also in more central parts of the nodules, distant from DR (Table 1). Our observations suggest the following steps of maturation during the metaplastic process: (i) initial expression of K7 in normally sized and arranged hepatocytes without association with ductules, (ii) gradual conversion of hepatocytes to the cholangiocytic phenotype along with progressive dissociation of plates by inflammation and fibrosis, (iii) appearance of K7/K19-positive ductules embedded in connective tissue, (iv) further maturation of DR to interlobular bile ducts may occur, but cannot be proved in our human material. Roskams et al.[37] reported the presence of undifferentiated progenitor cells in FNH on the basis of immunohistochemical (positivity for K7, K19, OV6, chromogranin A, NCAM) and electron-microscopic features, suggesting that progenitor cell activation also contributes to DR. Single or small clusters of K7-negative hepatocytes adjacent to cholangiocytes in fibrous septa, as observed by us in some areas of FNH, are similar to hepatocyte buds described in cirrhosis by Stueck and Wanless[12] and may also point to progenitor cell origin.

The pronounced expression of the senescence markers p21 and p16 in hepatocytes and cholangiocytes of FNH may provide pathogenic hints. However, it has been suggested that p21 expression may be limited to the onset of senescence and does not necessarily persist in senescent cells. Since p21 is also induced during transient cell cycle arrest in response to DNA damage, it should be regarded as a true senescence marker only in combination with other markers[20,21]. Persistent stress can activate p16, contributing to a long-lasting mitotic arrest. p16 is usually upregulated weeks after the induction of cell cycle arrest and persists for a longer time period. Therefore, p16 is regarded as one

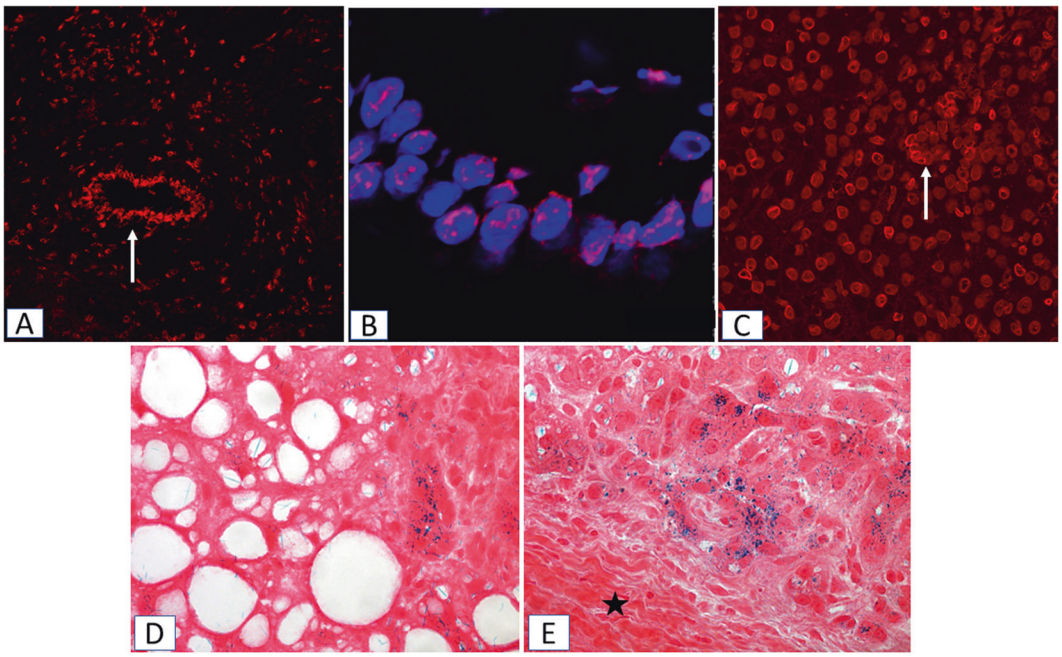

Fig. 7 Demonstration of γ-H2AX, lamin B1, SA β-galactosidase activity in FNH. FNH: Immunofluorescence microscopy using antibodies to γ-H2AX (**A**, **B**) and to lamin B1 (**C**). **A** Expression of γ-H2AX predominantly in nuclei of ductules (arrow). **B** Higher magnification of the DAPI-stained section: the nuclear location of γ-H2AX in the ductular cholangiocytes (red granules in blue background) is evident. **C** Expression of lamin B1 in nuclei of cholangiocytes (arrow) and hepatocytes. **D**, **E** Activity of SA-β-galactosidase in FNH is indicated by the blue granular precipitates restricted to ductular cholangiocytes. Steatotic hepatocytes in the neighbourhood (**D**) and connective tissue (asterisk in **E**) are negative.

of the most specific markers of senescence. But its use as an in vivo biomarker has also limitations, since p16-independent senescence can occur in vitro, and eventually p16 may also be expressed by non-senescent cells[20,21,38–40].

Does the expression of p16 and of p21 in hepatocytes and in the DR of FNH indicate cellular senescence, possibly resulting from oxidative stress caused by hyperoxygenation?

Several facts support this idea: (i) despite limitations mentioned above, p16 and p21 still remain acceptable senescence markers in vivo, particularly if present in combination; (ii) NCAM, which is expressed in the ductules of FNH (also shown by Roskams et al.[37]), is also associated with cellular senescence[41,42]; (iii) hyperoxygenation resulting from arterial hyperperfusion in FNH is a source of chronic oxidative stress and an important senescence inducer; nuclear γ-H2AX positivity of DR cells indicates the presence of a DNA damage response; (iv) expression of p16 in the DR of FNH is associated with inflammation and fibrosis, which can be attributed to components of the senescence-associated secretory phenotype (SASP) regulated by NF-κB target genes, i.e. proinflammatory cytokines (IL-6, TGF-β1) and chemokines that activate hepatic stellate cells[21,40]; a close link between activation of stellate cells and fibrosis in the septa and scars of FNH has been demonstrated[43]. (v) Senescent cholangiocytes are described in chronic biliary disorders[29,41–44]. Therefore, cholestasis could also contribute to senescence in FNH. Of note, p16 positivity of MDBs points to the role of senescence for the development of these inclusions. However, loss of lamin B1, which has also been reported as senescence-associated marker[45], was not observed in our studies. This could be due to the well-known heterogeneity of senescent phenotypes in different pathologic situations[20,21].

In view of the expression of senescence markers, usually in association with replicative arrest, the rare expression of the proliferation marker Ki-67 in FNH-associated hepatocytes and cholangiocytes was not surprising. Our results confirm Nolte et al. who also reported very low nuclear Ki-67 immunostaining in FNH[46].

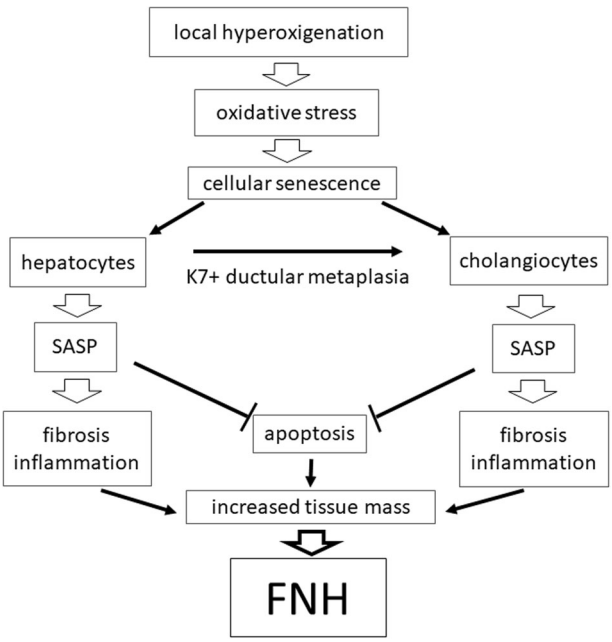

Fig. 8 Proposed mechanism of FNH development: local hyperoxygenation and oxidative stress induce senescence in hepatocytes and cholangiocytes. Transdifferentiation of hepatocytes to cholangiocytes may occur in combination with K7 expression and ductular metaplasia. The SASP responsible for fibrosis and inflammation while inhibiting apoptosis is leading to increased tissue volume observed in FNH, without necessitating increased proliferation.

The low Ki-67 and PCNA expression in DR as well as in hepatocytes of FNH is not in line with the usual definition of hyperplasia as an increase in tissue volume due to increased cell number caused by mitotic division. However, this finding is in

accordance with ductular metaplasia since K7-positive hepatocytes present in various types of liver diseases lack proliferation[47].

In conclusion, we provide evidence that FNH is associated with cellular senescence of hepatocytes and cholangiocytes. K7 positivity of hepatocytes as well as senescence of hepatocytes and cholangiocytes could be regarded as indicators of progression of the fibrosing and inflammatory process as described in other chronic liver diseases[8,26,27,33,40,48]. Moreover, since senescence is accompanied by resistance to apoptosis[21,40], the lack of apoptotic cell drop-out together with increased fibrosis and inflammation as a result of the SASP could instead of proliferation be responsible for the increased tissue volume and tumour-like appearance of the lesion (Fig. 8). Activation of progenitor cells may, in addition, be a contributing factor. In the DR also ductules with patent lumina lined by cuboidal epithelium were observed which are reminiscent of interlobular bile ducts. We, therefore, speculate that the occasional regression observed in aged FNH could result from dissection of nodules by newly developed septa, appearance of regular portal tracts via maturation of DR to interlobular bile ducts, and thus gradual restoration of normal liver architecture.

DATA AVAILABILITY

All data are contained in the paper and the Supplementary Material.

REFERENCES

1. Wanless, I. R., Mawdsley, C. & Adams, R. On the pathogenesis of focal nodular hyperplasia of the liver. *Hepatology* **5**, 1194–1200 (1985).
2. Ishak, K. G., Goodman, Z. D. & Stocker, J. T. Tumors of the liver and intrahepatic bile ducts. In: *Atlas of tumor pathology* 30–39 (Armed Forces Institute of Pathology: Washington, 1999).
3. Goodman, Z. D. & Terraciano, L. Focal nodular hyperplasia. In: Burt, A. D., Portmann, P. C. & Ferrell, L. D. (eds). *MacSween's Pathology of the Liver* (Elsevier, 2007).
4. Rebouissou, S., Bioulac-Sage, P. & Zucman-Rossi, J. Molecular pathogenesis of focal nodular hyperplasia and hepatocellular adenoma. *J. Hepatol.* **48**, 163–170 (2008).
5. Roncalli, M., Sciarra, A. & Tommaso, L. D. Benign hepatocellular nodules of healthy liver: focal nodular hyperplasia and hepatocellular adenoma. *Clin. Mol. Hepatol.* **22**, 199–211 (2016).
6. Balabaud, C. et al. Focal nodular hyperplasia and hepatocellular adenoma around the world viewed through the scope of the immunopathological classification. *Int. J. Hepatol*. 268625 https://doi.org/10.1155/2013/268625 (2013).
7. Paradis, V. et al. A quantitative gene expression study suggests a role for angiopoietins in focal nodular hyperplasia. *Gastroenterology* **124**, 651–659 (2003).
8. Yabushita, K. et al. Aberrant expression of cytokeratin 7 as a histological marker of progression in primary biliary cirrhosis. *Liver* **21**, 50–55 (2001).
9. Bankhead, P. et al. QuPath: open source software for digital pathology image analysis. *Sci. Rep.* **7**, 16878 (2017).
10. Team, R. C. R. *A Language and Environment for Statistical Computing*. (R Foundation for Statistical Computing, Vienna, Austria, 2019).
11. pastecs: Package for Analysis ofSpace-Time Ecological Series v. 1.3.21 (2018).
12. Stueck, A. E. & Wanless, I. R. Hepatocyte buds derived from progenitor cells repopulate regions of parenchymal extinction in human cirrhosis. *Hepatology* **61**, 1696–1707 (2015).
13. Jorgensen, M. A stereological study of intrahepatic bile ducts. 2. Bile duct proliferation in some pathological conditions. *Acta Pathol. Microbiol. Scand A* **81**, 663–669 (1973).
14. Desmet, V. J. The amazing universe of hepatic microstructure. *Hepatology* **50**, 333–344 (2009).
15. Desmet, V. J. Ductal plates in hepatic ductular reactions. Hypothesis and implications. I. Types of ductular reaction reconsidered. *Virchows Arch.* **3**, 251–259 (2011).
16. Schaub, J. R. et al. De novo formation of the biliary system by TGFbeta-mediated hepatocyte transdifferentiation. *Nature* **557**, 247–251 (2018).
17. van Eyken, P., Sciot, R., Callea, F. & Desmet, V. J. A cytokeratin-immunohistochemical study of focal nodular hyperplasia of the liver: further evidence that ductular metaplasia of hepatocytes contributes to ductular "proliferation". *Liver* **9**, 372–377 (1989).
18. Fischer, H. P. & Zhou, H. [Nodular lesions of liver parenchyma caused by pathological vascularisation/perfusion]. *Pathologe* **27**, 273–283 (2006).
19. Sato, Y. et al. Hepatic stellate cells are activated around central scars of focal nodular hyperplasia of the liver–a potential mechanism of central scar formation. *Hum. Pathol.* **40**, 181–188 (2009).
20. He, S. & Sharpless, N. E. Senescence in Health and Disease. *Cell* **6**, 1000–1011 (2017).
21. Herranz, N. & Gil, J. Mechanisms and functions of cellular senescence. *J. Clin. Invest.* **4**, 1238–1246 (2018).
22. Fischer, H. P., Meybehm, M., Zhou, H. & Schoch, J. [Hepatic neoductules]. *Verh Dtsch Ges. Pathol.* **79**, 36–46 (1995).
23. Roskams, T. A. et al. Nomenclature of the finer branches of the biliary tree: canals, ductules, and ductular reactions in human livers. *Hepatology* **39**, 1739–1745 (2004).
24. Richardson, M. M. et al. Progressive fibrosis in nonalcoholic steatohepatitis: association with altered regeneration and a ductular reaction. *Gastroenterology* **133**, 80–90 (2007).
25. Gouw, A. S., Clouston, A. D. & Theise, N. D. Ductular reactions in human liver: diversity at the interface. *Hepatology* **54**, 1853–1863 (2011).
26. Rokusz, A. et al. Ductular reaction correlates with fibrogenesis but does not contribute to liver regeneration in experimental fibrosis models. *PLoS ONE* **12**, e0176518 (2017).
27. Aguilar-Bravo, B. et al. Ductular reaction cells display an inflammatory profile and recruit neutrophils in alcoholic hepatitis. *Hepatology* **69**, 2180–2195 (2019).
28. Sato, K. et al. Ductular reaction in liver diseases: pathological mechanisms and translational significances. *Hepatology* **69**, 420–430 (2019).
29. Guicciardi, M. E., Trussoni, C. E., LaRusso, N. F. & Gores, G. J. The spectrum of reactive cholangiocytes in primary sclerosing cholangitis. *Hepatology* **71**, 741–748 (2020).
30. Strazzabosco, M. & Fabris, L. Development of the bile ducts: essentials for the clinical hepatologist. *J. Hepatol.* **56**, 1159–1170 (2012).
31. Fischer, H. P. & Lankes, G. Morphologic correlation between liver epithelium and mesenchyme allows insight into histogenesis of focal nodular hyperplasia (FNH) of the liver. *Virchows Arch B Cell Pathol. Incl. Mol. Pathol.* **60**, 373–380 (1991).
32. Michalopoulos, G. K., Bowen, W. C., Mule, K., Lopez-Talavera, J. C. & Mars, W. Hepatocytes undergo phenotypic transformation to biliary epithelium in organoid cultures. *Hepatology* **36**, 278–283 (2002).
33. Ren, C., Paronetto, F., Mak, K. M., Leo, M. A. & Lieber, C. S. Cytokeratin 7 staining of hepatocytes predicts progression to more severe fibrosis in alcohol-fed baboons. *J. Hepatol.* **38**, 770–775 (2003).
34. Sekiya, S. & Suzuki, A. Hepatocytes, rather than cholangiocytes, can be the major source of primitive ductules in the chronically injured mouse liver. *Am J. Pathol.* **184**, 1468–1478 (2014).
35. Nagahama, Y. et al. Contributions of hepatocytes and bile ductular cells in ductular reactions and remodeling of the biliary system after chronic liver injury. *Am J. Pathol.* **184**, 3001–3012 (2014).
36. Iyer, A., Robert, M. E., Bifulco, C. B., Salem, R. R. & Jain, D. Different cytokeratin and neuronal cell adhesion molecule staining patterns in focal nodular hyperplasia and hepatic adenoma and their significance. *Hum. Pathol.* **39**, 1370–1377 (2008).
37. Roskams, T., De Vos, R. & Desmet, V. 'Undifferentiated progenitor cells' in focal nodular hyperplasia of the liver. *Histopathology* **28**, 291–299 (1996).
38. Aravinthan, A. et al. Hepatocyte expression of the senescence marker p21 is linked to fibrosis and an adverse liver-related outcome in alcohol-related liver disease. *PLoS ONE* **8**, e72904 (2013).
39. Sharpless, N. E. & Sherr, C. J. Forging a signature of in vivo senescence. *Nat. Rev. Cancer* **15**, 397–408 (2015).
40. Aravinthan, A. D. & Alexander, G. J. M. Senescence in chronic liver disease: is the future in aging? *J. Hepatol.* **65**, 825–834 (2016).
41. Chiba, M. et al. Participation of bile ductular cells in the pathological progression of non-alcoholic fatty liver disease. *J. Clin. Pathol.* **64**, 564–570 (2011).
42. Sasaki, M. et al. Bile ductular cells undergoing cellular senescence increase in chronic liver diseases along with fibrous progression. *Am J. Clin. Pathol.* **133**, 212–223 (2010).
43. Sato, K., Meng, F., Glaser, S. & Alpini, G. Cellular Senescence in Cholestatic Liver Injury. *J. Experimen. Res. Hum. Growth Aging* **1**, 1–6 (2018).
44. Tabibian, J. H., O'Hara, S. P., Splinter, P. L., Trussoni, C. E. & LaRusso, N. F. Cholangiocyte senescence by way of N-ras activation is a characteristic of primary sclerosing cholangitis. *Hepatology* **59**, 2263–2275 (2014).
45. Freund, A., Laberge, R. M., Demaria, M. & Campisi, J. Lamin B1 loss is a senescence-associated biomarker. *Mol. Biol. Cell* **23**, 2066–2075 (2012).
46. Nolte, M. et al. Expression of proliferation associated antigens and detection of numerical chromosome aberrations in primary human liver tumours: relevance to tumour characteristics and prognosis. *J. Clin. Pathol.* **51**, 47–51 (1998).

47. Delladetsima, I., Sakellariou, S., Kokkori, A. & Tiniakos, D. Atrophic hepatocytes express keratin 7 in ischemia-associated liver lesions. *Histol. Histopathol.* **31**, 1089–1094 (2016).
48. Papatheodoridi, A. M., Chrysavgis, L., Koutsilieris, M. & Chatzigeorgiou, A. The role of senescence in the development of nonalcoholic fatty liver disease and progression to nonalcoholic steatohepatitis. *Hepatology* **71**, 363–374 (2020).

AUTHOR CONTRIBUTIONS

H.D., P.M.A., K.Z., C.L.: design and discussion of the topic. H.D., C.L.: assessment of sections. H.D., P.M.A.: preparation of the manuscript. R.R.: statistics. D.P., B.T.: technical assistance, methodology.

COMPETING INTERESTS

The authors declare no competing interests.

ETHICS APPROVAL

The study was approved by the Ethics Committee of the Medical University of Graz, Austria (Ref. No. 20-119 ex 08/09).

ADDITIONAL INFORMATION

Supplementary information The online version contains supplementary material available at https://doi.org/10.1038/s41379-021-00940-5.

Correspondence and requests for materials should be addressed to Helmut Denk.

Reprints and permission information is available at http://www.nature.com/reprints

Publisher's note Springer Nature remains neutral with regard to jurisdictional claims in published maps and institutional affiliations.